

# Shell model description of $^{16}\text{O}(p,\gamma)^{17}\text{F}$ and $^{16}\text{O}(p,p)^{16}\text{O}$ reactions

K. Bennaceur<sup>1,2</sup>, N. Michel<sup>1</sup>, F. Nowacki<sup>3</sup>, J. Okołowicz<sup>1,4</sup> and M. Płoszajczak<sup>1</sup>

1. *Grand Accélérateur National d'Ions Lourds (GANIL), CEA/DSM – CNRS/IN2P3, BP 5027,*

*F-14076 Caen Cedex 05, France*

2. *Centre d'Etudes de Bruyères-le-Châtel, BP 12, F-91680 Bruyères-le-Châtel, France*

3. *Laboratoire de Physique Théorique Strasbourg (EP 106), 3-5 rue de l'Université, F-67084*

*Strasbourg Cedex, France*

4. *Institute of Nuclear Physics, Radzikowskiego 152, PL - 31342 Krakow, Poland*

## Abstract

We present shell model calculations of both the structure of  $^{17}\text{F}$  and the reactions  $^{16}\text{O}(p,\gamma)^{17}\text{F}$ ,  $^{16}\text{O}(p,p)^{16}\text{O}$ . We use the ZBM interaction which provides a fair description of the properties of  $^{16}\text{O}$  and neighbouring nuclei and, in particular it takes account for the complicated correlations in coexisting low-lying states of  $^{16}\text{O}$ .

21.60.Cs, 24.10.Eq, 25.40.Lw, 27.20.+n

A realistic account of the low-lying states properties in exotic nuclei requires taking into account the coupling between discrete and continuum states which is responsible for unusual spatial features of these nuclei. Within the newly developed Shell Model Embedded in the Continuum (SMEC) approach [1], one may obtain the unified description of the divergent characteristics of these states as well as the reactions involving one-nucleon in the continuum. This provides a stringent test of approximations involved in the SMEC calculations and permits to assess the mutual complementarity of the reaction and structure data for understanding of these nuclei. The quality of the SMEC description depends crucially on the realistic account of the configuration mixing for coexisting low-lying structures and hence on the quality of the Shell Model (SM) effective interactions and the SM space considered. In this work, we shall present the calculation for  $^{17}\text{F}$  for which it is believed that configurations of up to four particles and four holes are necessary. Closed shell nuclei are never inert and multiple particle-hole excitations are always observed in their spectra. In  $^{16}\text{O}$  and  $^{17}\text{O}$ , Brown and Green described the low-lying spectra by mixing spherical and deformed states [2]. From the shell model point of view, Zuker-Buck-McGrory (ZBM) set an effective interaction in the basis of  $0p_{1/2}$ ,  $1s_{1/2}$  and  $0d_{5/2}$  orbitals [3,4]. This valence space has the advantage to be practically non spurious and most of states at the  $p - sd$  interface around  $^{16}\text{O}$  are nicely described through configuration mixing of these three orbitals. In particular, the energy spectra, spectroscopic factors and correlations in the low-lying states of  $A = 16$  and  $A = 17$  nuclei are well reproduced [5]. The wavefunction components for the first three  $0^+$  states in  $^{16}\text{O}$  are in a fair agreement with the recently developed interactions in the full  $p - sd$  shells [6]. The aim of this work is not to provide better new SM wavefunctions for  $^{16}\text{O}$  but to build on them the continuum effects and to investigate the consequences of this coupling both for the structure of  $^{17}\text{F}$  and for the reactions  $^{16}\text{O}(p,\gamma)^{17}\text{F}$ ,  $^{16}\text{O}(p,p)^{16}\text{O}$ . For that purpose, the ZBM interaction is satisfactory and we are going to use it in this study.

In the SMEC formalism the subspaces of (quasi-) bound (the  $Q$  subspace) and scattering (the  $P$  subspace) states are not separated artificially [1]. (For the review of earlier works see also Ref. [7]). Using the projection operator technique, we separate the  $P$  subspace of asymptotic channels from the  $Q$  subspace of many-body localized states which are build up by the bound single-particle (s.p.) wavefunctions and by the s.p. resonance wavefunctions.  $P$  subspace contains  $(N - 1)$ -particle localized states and one nucleon in the scattering state. The s.p. resonance wavefunctions outside of the cutoff radius  $R_{cut}$  are included in the  $P$  subspace. The resonance wavefunctions for  $r < R_{cut}$  are included in the  $Q$  subspace. The wavefunctions in  $Q$  and  $P$  are then properly renormalized in order to ensure the orthogonality of wavefunctions in both subspaces.

In the first step, we calculate the (quasi-) bound many-body states in  $Q$  subspace. For that we solve the multiconfigurational SM problem :  $H_{QQ}\Phi_i = E_i\Phi_i$ , using the code ANTOINE [8]. For  $H_{QQ} \equiv QHQ$  we take the ZBM interaction which yields realistic *internal mixing* of many-body configurations in  $Q$  subspace.

To generate the radial s.p. wavefunctions in  $Q$  subspace and the scattering wavefunctions in  $P$  subspace we use the average potential of Woods-Saxon (WS) type with the spin-orbit and Coulomb parts included:

$$U(r) = V_0f(r) + V_{SO}\lambda_\pi^2(2\mathbf{l} \cdot \mathbf{s})\frac{1}{r}\frac{df(r)}{dr} + V_C ,$$

where  $\lambda_\pi^2 = 2\text{fm}^2$  is the pion Compton wavelength and  $f(r)$  is the spherically symmetrical

WS formfactor :  $f(r) = [1 + \exp((r - R_0)/a)]^{-1}$ . The Coulomb potential  $V_C$  is calculated for the uniformly charged sphere with radius  $R_0$ . This 'first guess' potential  $U(r)$ , is then modified by the residual interaction. We shall return to this problem below.

For the continuum part, we solve the coupled channel equations :

$$(E^{(+)} - H_{PP})\xi_E^{c(+)} \equiv \sum_{c'} (E^{(+)} - H_{cc'})\xi_E^{c'(+)} = 0 ,$$

where index  $c$  denotes different channels and  $H_{PP} \equiv PHP$ . The superscript (+) means that boundary conditions for incoming wave in the channel  $c$  and outgoing scattering waves in all channels are used. The channel states are defined by coupling of one nucleon in the scattering continuum to the many-body SM state in  $(N - 1)$ -nucleus. For the coupling between bound and scattering states around  $^{16}\text{O}$ , we use the density dependent interaction which is close to the Landau - Migdal type of interactions [9,10]. However, as compared to the original force of Schwesinger and Wambach [9], the radius parameter  $r_0$  of the WS density formfactor is somewhat reduced to better fit the experimental matter radius in oxygen ( $r_0 = 2.64$  fm). This interaction provides *external mixing* of SM configurations via the virtual excitations of particles to the continuum states.

The channel - channel coupling potential is :

$$H_{cc'} = (T + U)\delta_{cc'} + v_{cc'}^J , \quad (1)$$

where  $T$  is the kinetic-energy operator and  $v_{cc'}^J$  is the channel-channel coupling generated by the residual interaction. Reduced matrix elements of the channel - channel coupling, which involve one-body operators of the kind :  $\mathcal{O}_{\beta\delta}^K = (a_{\beta}^{\dagger}\tilde{a}_{\delta})^K$ , depend sensibly on the amount of  $2p - 2h$  and  $4p - 4h$  correlations in the ground state of  $^{16}\text{O}$ . The potential for channel  $c$  in (1) consists of initial WS guess,  $U(r)$ , and of the diagonal part of coupling potential  $v_{cc}^J$  which depends on both the s.p. orbit  $\phi_{l,j}$  and the considered many-body state  $J^{\pi}$ . This modification of the initial potential  $U(r)$  change the generated s.p. wavefunctions  $\phi_{l,j}$  defining  $Q$  subspace which in turn modify the diagonal part of the residual force, *etc.* In other words, the procedure of solving of the coupled channel equations is accompanied by the self-consistent iterative procedure which yields for each total  $J$  independently the new self-consistent potential :

$$U^{(sc)}(r) = U(r) + v_{cc}^{J(sc)}(r) ,$$

and consistent with it the new renormalized formfactor of the coupling force.  $U^{(sc)}(r)$  differs significantly from the initial WS potential, especially in the interior of the potential [1,10]. Parameters of  $U(r)$  are chosen in such a way that  $U^{(sc)}(r)$  reproduces energies of experimental s.p. states, whenever their identification is possible.

The third system of equations in SMEC consists of the inhomogeneous coupled channel equations:

$$(E^{(+)} - H_{PP})\omega_i^{(+)} = H_{PQ}\Phi_i \equiv w_i$$

with the source term  $w_i$  which depends on the structure of  $N$  - particle SM wavefunction  $\Phi_i$ . Formfactor of the source term is given by the self-consistently determined s.p. wavefunctions. The solutions :  $\omega_i^{(+)} \equiv G_P^{(+)}H_{PQ}\Phi_i$ , where  $G_P^{(+)}$  is the Green function for the motion of s.p. in the  $P$  subspace, describe the decay of quasi-bound state  $\Phi_i$  in the continuum. Reduced matrix elements of the source term, which involve products of two annihilation operators

and one creation operator of the kind :  $\mathcal{R}_{\gamma\delta(L)\beta}^{j\alpha} = (a_{\beta}^{\dagger}(\tilde{a}_{\gamma}\tilde{a}_{\delta})^L)^{j\alpha}$ , are calculated between different initial state wavefunctions in  $^{17}\text{F}$  and a given final state wavefunction in  $^{16}\text{O}$ . It should be stressed that the matrix elements of the source term depend sensitively on the percentage of the shell closure in  $^{16}\text{O}$ , *i.e.*, on the amount of correlations both in the g.s. of  $^{16}\text{O}$  and in the considered states of  $^{17}\text{F}$ . Obviously, this kind of couplings are not accounted for by the spectroscopic amplitudes.

The total wavefunction is expressed by three functions:  $\Phi_i$ ,  $\xi_E^c$  and  $\omega_i$  [1,7] :

$$\Psi_E^c = \xi_E^c + \sum_{i,j} (\Phi_i + \omega_i) \frac{1}{E - H_{QQ}^{eff}} \langle \Phi_j | H_{QP} | \xi_E^c \rangle \quad (2)$$

where :  $H_{QQ}^{eff}(E) = H_{QQ} + H_{QP}G_P^{(+)}H_{PQ}$ , is the new energy dependent effective SM Hamiltonian which contains the coupling to the continuum. Operator  $H_{QQ}^{eff}(E)$ , which is Hermitian for energies below the particle emission threshold, becomes non-Hermitian for energies higher than the threshold. Consequently, the eigenvalues  $\tilde{E}_i - \frac{1}{2}i\tilde{\Gamma}_i$  are complex for decaying states and depend on the energy  $E$  of the particle in the continuum. The energy and the width of resonance states are determined by the condition:  $\tilde{E}_i(E) = E$ . The eigenstates corresponding to these eigenvalues can be obtained by the orthogonal but in general non-unitary transformation [7,10]. Inserting them in (2), one obtains symmetrically the new continuum many-body wavefunctions modified by the discrete states, and the new discrete state wavefunctions modified by the coupling to the continuum states.

The SMEC wavefunctions, can be used to calculate various spectroscopic and reaction quantities. These include for example the proton (neutron) capture data, Coulomb dissociation data, elastic (inelastic) proton (neutron) scattering data, energies and wavefunctions of discrete and resonance states, transition matrix elements between SMEC wavefunctions, static nuclear moments *etc.* [1,10,11]. The application of the SMEC model for the description of structure for mirror nuclei and capture cross sections for mirror reactions in  $p$ -shell has been published in Ref. [1]. The analysis of the structure of  $^{17}\text{F}$  and the reactions  $^{16}\text{O}(p, \gamma)^{17}\text{F}$ ,  $^{16}\text{O}(p,p)^{16}\text{O}$  in the  $(0p1s0d)$ -space, *neglecting* the 2p-2h, 4p-4h admixtures in  $^{16}\text{O}$  wavefunctions have been reported recently as well [10]. To correct for the missing correlations in the low-energy wavefunctions of  $^{16}\text{O}$  and  $^{17}\text{F}$ , the matrix elements of the  $Q - P$  coupling in this study [10] have been quenched by the factors related to the spectroscopic amplitudes for positive parity states in  $^{17}\text{F}$  ( $^{17}\text{O}$ ) and to the amount of  $2p - 2h$ ,  $4p - 4h$  correlations in the g.s. of  $^{16}\text{O}$ . This quenching correction of the effective operator allowed to obtain a reasonable description of the spectrum of  $^{17}\text{F}$  but failed in solving the problem of 'halo' of discrete states for positive energies which was observed in the elastic cross section and in the phase shifts [10]. The whole problem results from the non-hermitean corrections to the eigenvalues for positive energies which generate the imaginary part and which are particularly large for pure single-particle (or single-hole) configurations. For this reason, the incorrect internal configuration mixing in SM wavefunctions may lead to an unphysical enhancement of the resonant-like correction from bound states into the scattering data (e.g. the elastic phase-shifts). This aspect of the continuum coupling we want to investigate using the ZBM interaction which includes the most essential for the present studies configuration mixing in low energy wavefunctions.

In Fig. 1 we show SMEC energies and widths for positive parity (l.h.s. of the plot) and negative parity (r.h.s. of the plot) states of  $^{17}\text{F}$ . The calculations were performed using either

the density dependent interaction of Ref. [9], called DDSM0, or the similar interaction with the overall strength reduced by a factor 0.67, called DDSM1 [10]. (In both cases, radius of the density formfactor has been reduced as discussed above.) This latter interaction was used before in the SMEC calculations in  $0p1s0d$  SM space [10]. However, since the external mixing of wavefunctions in the SM space of ZBM is smaller than in the  $0p1s0d$  SM space, therefore one may consider bigger coupling strength of the residual interaction in SMEC-ZBM calculations. For that reason, we compare results obtained with both DDSM0 and DDSM1 interactions. For the comparison, the experimental data and the SM input in  $Q$ -space is shown in Fig. 1 separately for positive and negative parity states as well. The agreement of the SM-ZBM calculations with the experimental data is even better than obtained in the  $0p1s0d$  SM space [10]. The agreement of SMEC calculations with experiment is encouraging for both density dependent interactions but the widths of states are better reproduced by SMEC-DDSM0. Only the coupling matrix elements between the  $J^\pi = 0_1^+$  g.s. wavefunction of  $^{16}\text{O}$  and all considered states in  $^{17}\text{F}$  are included. Zero of the energy scale for  $^{17}\text{F}$  is fixed by the experimental position of  $J^\pi = 1/2_1^+$  ( $E = -105$  keV) with respect to the proton emission threshold. In Fig. 1 the theoretical prediction for  $3/2^+$  state is compared with the experimental  $3/2_2^+$  state, because the s.p. orbit  $0d_{3/2}$  is missing in SM space of ZBM. For those s.p. wavefunctions which in a given many body state are not modified by the selfconsistent renormalization, we calculate radial formfactors using the common reference s.p. potential  $U^{(ref)}$  of the WS type which is adjusted to reproduce experimental binding energies of  $5/2_1^+$  and  $1/2_1^+$  states for protons [10]. This potential has the following parameters: the radius  $R_0 = 3.214$  fm, the diffuseness  $a = 0.58$  fm, the spin-orbit strength  $V_{SO} = 3.683$  MeV and the depth  $V_0 = -52.46$  MeV. The same potential without the Coulomb term is also used to calculate radial formfactors for neutrons. In the case when the self-consistent conditions in a  $J^\pi$  state determine the radial function of a s.p. wavefunction  $\phi_{l,j}$ , we readjust the depth of 'first guess' potential  $U(r)$  so that the energy of the s.p. state  $\phi_{l,j}$  in the converged potential  $U^{(sc)}(r)$  corresponds to the energy of this s.p. state in  $U^{(ref)}$ . The remaining parameters:  $R_0$ ,  $a$ ,  $V_{SO}$ , of the initial potential are the same as in the reference potential  $U^{(ref)}$ . This readjustment of  $V_0$  in the initial potentials  $U(J^\pi)$  for a s.p. state  $(l,j)$  guarantees that the binding of self-consistently determined wavefunction  $\phi_{l,j}$  is at the experimental value. Moreover, we have the same s.p. energies and, consequently, the same asymptotic behaviours of wavefunctions for large  $r$  for both residual density dependent interactions. This choice is essential for quantitative description of radiative capture cross-section.

$B(E2)$  transition matrix element between  $1/2_1^+$  and  $5/2_1^+$  bound states is an interesting test of the wavefunction. In SMEC with ZBM interaction and DDSM0 residual coupling, the value for this transition:  $B(E2) = 79.61$  e<sup>2</sup>fm<sup>4</sup>, which is obtained assuming the effective charges:  $e_p \equiv 1 + \delta_p$ ,  $e_n \equiv \delta_n$ , with the polarization charge  $\delta = \delta_p = \delta_n = 0.2$ , agrees with the experimental value  $B(E2)_{exp} = 64.92$  e<sup>2</sup>fm<sup>4</sup>. For the range of  $\delta$  in between 0.1 and 0.3, which is compatible with the theoretical estimates [12], the SM values with Harmonic Oscillator wavefunctions are much smaller. This difference reflects a more realistic radial dependence of the  $1s_{1/2}$  s.p. orbit in  $J^\pi = 1/2_1^+$  many body state which is in part a consequence of the external mixing in SMEC wavefunctions due to the coupling to the scattering continuum and provides the halo structure of the  $1s_{1/2}$  s.p. orbit. Similar effect can be generated using the WS potential or Pöschl-Teller-Ginocchio potential for the appropriately chosen  $1s_{1/2}$

orbit [13]. The rms radius for this orbit in SMEC is :  $\langle r^2 \rangle^{1/2} = 5.24$  fm, as compared to :  $\langle r^2 \rangle^{1/2} = 3.03$  fm in SM.

In Fig. 2, the calculated total astrophysical  $S$ -factor as a function of the c.m. energy, as well as its values for the  $^{16}\text{O}(p, \gamma)^{17}\text{F}(J^\pi = 1/2_1^+)$  and  $^{16}\text{O}(p, \gamma)^{17}\text{F}(J^\pi = 5/2_1^+)$  branches are compared with the experimental data [14]. Results shown in Fig. 2 have been calculated with DDSM1 interaction. The total  $S$ -factor depends weakly on the strength of the residual coupling and with DDSM0 interactions one obtains very similar results. The energy scale is adjusted to reproduce the experimental position of  $1/2_1^+$  state with respect to the proton emission threshold. Therefore, the energy scale for excitation energy is the same as c.m. energy in the  $p + ^{16}\text{O}$  system. The photon energy is then given by the difference of c.m. energy of  $[^{16}\text{O} + p]_{J_i}$  system and the experimental energy of the final state  $J_f$  in  $^{17}\text{F}$ . The dominant contribution to the total capture cross-section for both  $5/2_1^+$  and  $1/2_1^+$  final states, is provided by  $E1$  transitions from the incoming  $p$  wave to the bound  $0d_{5/2}$  and  $1s_{1/2}$  states. We took into account all possible  $E1$ ,  $E2$ , and  $M1$  transitions from incoming  $s$ ,  $p$ ,  $d$ ,  $f$ , and  $g$  waves but only  $E1$  from incoming  $p$ -waves give important contributions. In the transition to the g.s., the  $E1$  contribution from incoming  $f_{7/2}$  wave is by a factor  $\sim 100$  smaller than the contribution from  $p_{3/2}$  wave at  $E_{CM} \sim 0$ . This contribution however increases with the energy of incoming proton and becomes  $\sim 0.3$  at 3.5 MeV.

The energy dependence of  $S$ -factor as  $E_{CM} \rightarrow 0$  can be fitted by a second order polynomial to calculated points obtained in the interval from 20 to 50 keV in steps of 1 keV. We have  $S(0) = 9.32 \times 10^{-3}$  MeV·b, and the logarithmic derivative is  $S'(0)/S(0) = -4.86$  MeV $^{-1}$ . These results have been obtained for DDSM1 residual interaction but are practically identical for the DDSM0 force. The ratio of  $E2$  and  $E1$  contributions in the branch  $^{16}\text{O}(p, \gamma)^{17}\text{F}(J^\pi = 1/2_1^+)$  for DDSM1 interaction is :  $\sigma^{E2}/\sigma^{E1} = 1.622 \times 10^{-4}$ ,  $2.225 \times 10^{-4}$  and  $5.458 \times 10^{-4}$  at 20, 100 and 500 keV, respectively. Also these ratios do not depend on the strength of the residual coupling. On the contrary, the ratio  $\sigma^{M1}/\sigma^{E1}$  depends on the residual coupling and equals  $3.90 \times 10^{-4}$  and  $1.087 \times 10^{-3}$  at  $E_{CM} \rightarrow 0$  for DDSM1 and DDSM0 interactions respectively. At 500 keV, this ratio equals  $6.11 \times 10^{-5}$  and  $1.81 \times 10^{-4}$  for both interactions, respectively.

For the deexcitation to the g.s.  $5/2_1^+$ , the fit of calculated  $S$ -factor for DDSM1 interaction as  $E_{CM} \rightarrow 0$  yields:  $S(0) = 3 \times 10^{-4}$  MeV·b and  $S'(0)/S(0) = 0.649$  MeV $^{-1}$ . Almost identical results are obtained with the DDSM0 interaction. The ratio of  $E2$  and  $E1$  contributions for DDSM1 interaction at 20, 100 and 500 keV is:  $\sigma^{E2}/\sigma^{E1} = 1.336 \times 10^{-3}$ ,  $1.11 \times 10^{-3}$  and  $9.74 \times 10^{-4}$ , respectively. These ratios show some sensitivity on the residual coupling. For DDSM0 one obtains :  $\sigma^{E2}/\sigma^{E1} = 2.25 \times 10^{-3}$ ,  $1.458 \times 10^{-3}$  and  $1.043 \times 10^{-3}$  at 20, 100 and 500 keV, respectively. Similarly as in the branch  $^{16}\text{O}(p, \gamma)^{17}\text{F}(J^\pi = 1/2_1^+)$ , the ratio  $\sigma^{M1}/\sigma^{E1}$  depends on the residual coupling and equals  $2 \times 10^{-3}$  and  $2.99 \times 10^{-3}$  at  $E_{CM} \rightarrow 0$  for DDSM1 and DDSM0 interactions respectively. In the total cross section, ratio of  $E2$  and  $E1$  contributions at 20, 100 and 500 keV equals :  $\sigma^{E2}/\sigma^{E1} = 2.03 \times 10^{-4}$ ,  $2.63 \times 10^{-4}$  and  $5.85 \times 10^{-4}$  for DDSM1 interaction, and  $\sigma^{E2}/\sigma^{E1} = 2.34 \times 10^{-4}$ ,  $2.8 \times 10^{-4}$  and  $5.92 \times 10^{-4}$  for DDSM0 interaction.

Elastic phase shifts and elastic cross-sections for different proton bombarding energies are shown in Figs. 3 and 4. The elastic phase shifts data [15] are very well reproduced by the SMEC calculations for all considered partial waves including the  $5/2^+$  for which a significant discrepancy with the data has been reported in SMEC calculations using the

$p$ - $sd$  interaction neglecting higher order  $p$ - $h$  correlations in the SM wavefunction for positive parity states [10]. In Fig. 3 we show the calculations for the DDSM1 residual interaction. As we have already mentioned,  $0d_{3/2}$  s.p. orbit is missing in the  $Q$  subspace. On the other hand, the  $3/2^+$  partial wave contributes to the elastic cross-section. So we have decided to include this resonance in the  $P$  subspace, adjusting scattering potential for the  $d_{3/2}$  proton wave to place it at the experimental position. The encouraging agreement of SMEC results with the data for the spectrum of  $^{17}\text{F}$ , the proton capture cross-section  $^{16}\text{O}(p, \gamma)^{17}\text{F}(J^\pi = 5/2_1^+)$  and the  $5/2^+$  elastic phase shift is not accidental and shows importance of the  $np$ - $nh$  excitations across the 'closed core'  $N = Z = 8$ , which are taken into account in the present studies with the ZBM force.

Calculated elastic excitation functions at a laboratory angle of  $166^\circ$  in SMEC with DDSM0 (the solid line) and DDSM1 (the dashed line) are compared with the experimental data [16] in Fig. 4. The agreement is very encouraging for both residual interactions in the almost entire energy range. where the interference pattern depending sensitively on the precise values of the energy and width of resonance states is absent. Earlier SMEC calculations [10], using the simplified wavefunctions for the g.s. of  $^{16}\text{O}$  and  $^{17}\text{F}$ , failed to reproduce the experimental elastic cross-section in the low-energy domain below the resonances. We have found that an unrealistic account for excitations from  $0p$  to  $1s0d$  shells leads to a large resonant contribution from the g.s.  $5/2_1^+$  wavefunction to the phase shift in the partial wave  $5/2^+$  and implies a strong decrease of the elastic excitation function at low energies. This effect is caused by the virtual coupling of discrete and continuum states. For energies below the proton emission threshold, coupling to the continuum introduces hermitean modifications of  $H_{QQ}$  which shift the energy of  $5/2_1^+$  state with respect to its initial position given by the SM but do not generate any width for this state. For excitation energies above the proton threshold, the  $Q - P$  coupling generates non-hermitean corrections which yield the imaginary part of the eigenvalue of  $H_{QQ}^{eff}$  and, hence, produce the resonant behavior. Internal mixing of configurations in the SM wavefunctions tend to reduce this resonant behavior for positive energies which, in general, is strongest for the states having little internal mixing, *i.e.* those having a s.p. nature. Actually, these strong resonant-like features associated with certain bound states for positive energies (above the particle-emission threshold) and the large shifts of the real part for certain eigenvalues at negative energies (below the particle-emission threshold), have the same origin in the interplay between external (*i.e.* via the continuum coupling) and internal (*i.e.* within  $Q$  space) configuration mixing in the SMEC wavefunction for this state. This example shows also that in the SMEC approach, one may use different experimental observables to fix those few parameters of the model such as the overall strength of the residual  $Q - P$  coupling or the radius and depth of the initial average potential. Moreover, the information about the amount of correlations in the low-lying coexisting states can be extracted not only from the spectroscopic data but also from the elastic excitation function. For nuclei far from the stability line where the amount of experimental data is strongly limited, this feature of the model is very attractive.

We feel that the evidence presented in this work shows that the SM calculation extended to include the coupling to the continuum of the scattering states can go a long way towards providing a detailed explanation not only of the structure of  $^{17}\text{F}$ ,  $^{16}\text{O}$  and neighboring nuclei, but also the reaction data involving one nucleon in the continuum. The corner-stone of this model is the effective SM interaction providing a realistic internal mixing of configurations

in the  $Q$  subspace. Several problems remain, such as the missing configurations and/or more realistic asymptotic decay channels which show up in the decay width of resonances. In this latter case, the extension of the SMEC is being investigated.

### **Acknowledgments**

We thank E. Caurier for his help in the early stage of development of SMEC model. This work was partly supported by KBN Grant No. 2 P03B 097 16 and the Grant No. 76044 of the French - Polish Cooperation.



## REFERENCES

- [1] K. Bennaceur, F. Nowacki, J. Okołowicz, and M. Płoszajczak, J. Phys. **G 24** (1998) 1631; Nucl. Phys. **A 651** (1999) 289.
- [2] G.E. Brown and A.M. Green, Nucl. Phys. **75** (1966) 401.
- [3] A.P. Zuker, B. Buck and J.B. McGrory, Phys. Rev. Lett. **21** (1968) 39.
- [4] A.P. Zuker, Phys. Rev. Lett. **23** (1969) 983.
- [5] The problem encountered by the ZBM interaction in describing  $B(E1)$  transition strength is of no importance in the present analysis.
- [6] W.C. Haxton and C. Johnson, Phys. Rev. Lett. **65** (1990) 1325; E.K. Warburton, B.A. Brown and D.J. Millener, Phys. Lett. **B 293** (1992) 7.
- [7] I. Rotter, Rep. Prog. Phys. **54** (1991) 635.
- [8] E. Caurier, code ANTOINE (unpublished).
- [9] B. Schwesinger and J. Wambach, Nucl. Phys. **A 426** (1984) 253.
- [10] K. Bennaceur, F. Nowacki, J. Okołowicz, and M. Płoszajczak, Nucl. Phys. **A 671** (2000) 203.
- [11] R. Shyam, K. Bennaceur, J. Okołowicz, and M. Płoszajczak, Nucl. Phys. **A 669** (2000) 65.
- [12] M.W. Kirson, Ann. Phys. (NY) **82** (1974) 345.
- [13] J.N. Ginocchio, Annals of Physics (NY) **152** (1984) 203; **159** (1985) 467; K. Bennaceur, J. Dobaczewski and M. Płoszajczak, Phys. Rev. **C 60** (1999) 034308.
- [14] R. Morlock, R. Kunz, A. Mayer, M. Jaeger, A. Müller, J.W. Hammer, P. Mohr, H. Oberhammer, G. Staudt, and V. Kölle, Phys. Rev. Lett. **79** (1997) 3837.
- [15] R.A. Blue and W. Haeberli, Phys. Rev. **137** (1965) B284.
- [16] S.R. Salisbury, G. Haradie, L. Oppliger, and R. Dangle, Phys. Rev. **126** (1962) 2143.

FIGURES

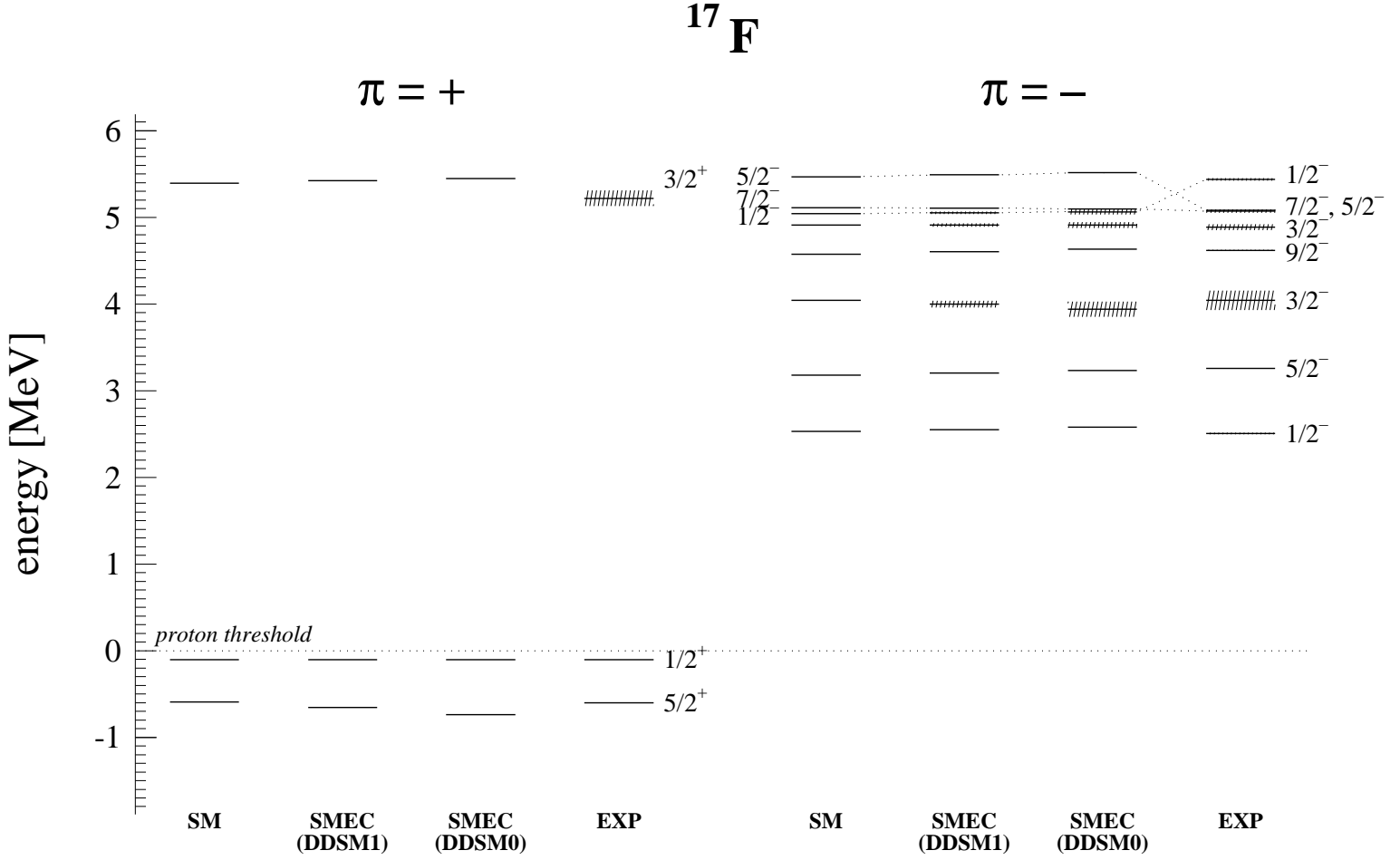


FIG. 1. SM and SMEC energy spectra obtained with the ZBM effective SM interaction [3,4] are compared with the experimental states of  $^{17}\text{F}$  nucleus. For the residual coupling between  $Q$  and  $P$  subspaces we use the density dependent DDSM0 [9] and DDSM1 [10] interactions. The proton threshold energy is adjusted to reproduce position of the  $1/2_1^+$  first excited state. The shaded regions represent the width of resonance states. For the details of the calculation see the description in the text.

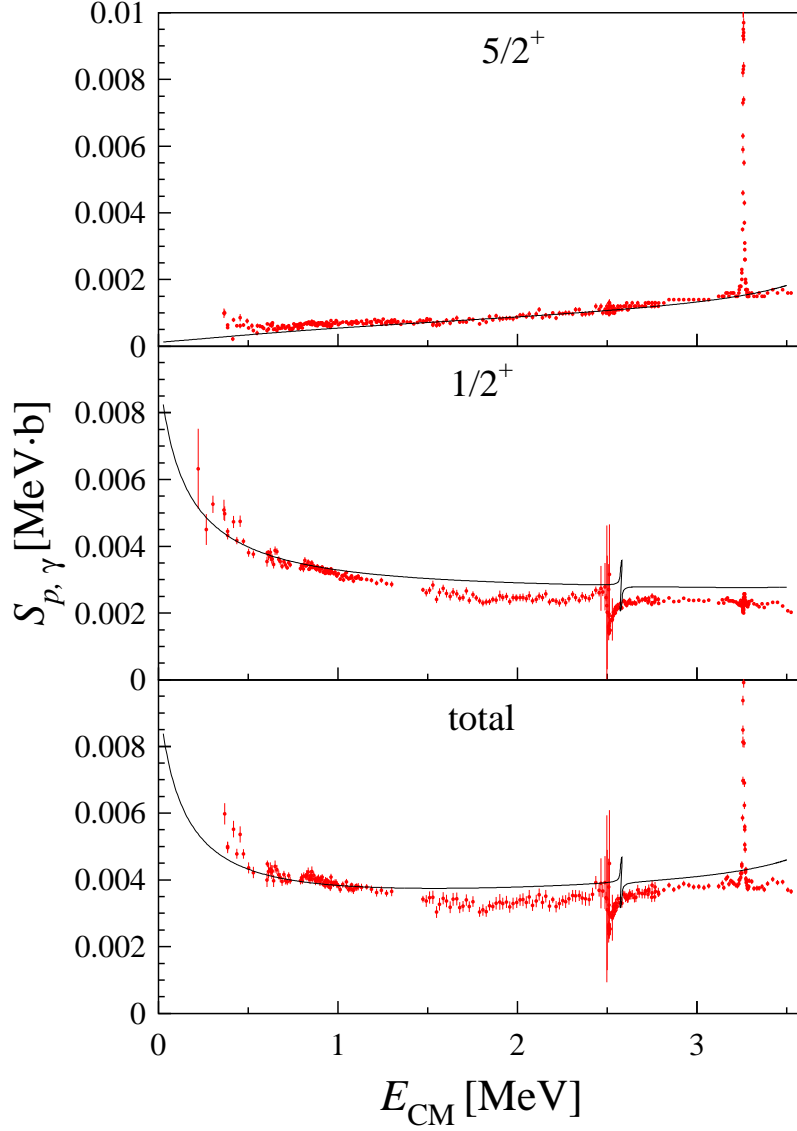


FIG. 2. The astrophysical  $S$ -factor for the reactions  $^{16}\text{O}(p,\gamma)^{17}\text{F}(J^\pi = 5/2_1^+)$  and  $^{16}\text{O}(p,\gamma)^{17}\text{F}(J^\pi = 1/2_1^+)$  is plotted as a function of the center of mass energy  $E_{CM}$ . For the residual coupling between  $Q$  and  $P$  subspaces we use DDSM1 density dependent interaction [10]. The experimental data are from [14]. The contribution of  $5/2_1^-$  resonance in the  $^{16}\text{O}(p,\gamma)^{17}\text{F}(J^\pi = 5/2_1^+)$  branch is very narrow in energy and has been omitted in the figure. The resonance is found at 5.29 MeV in the SMEC-DDSM1 calculations.

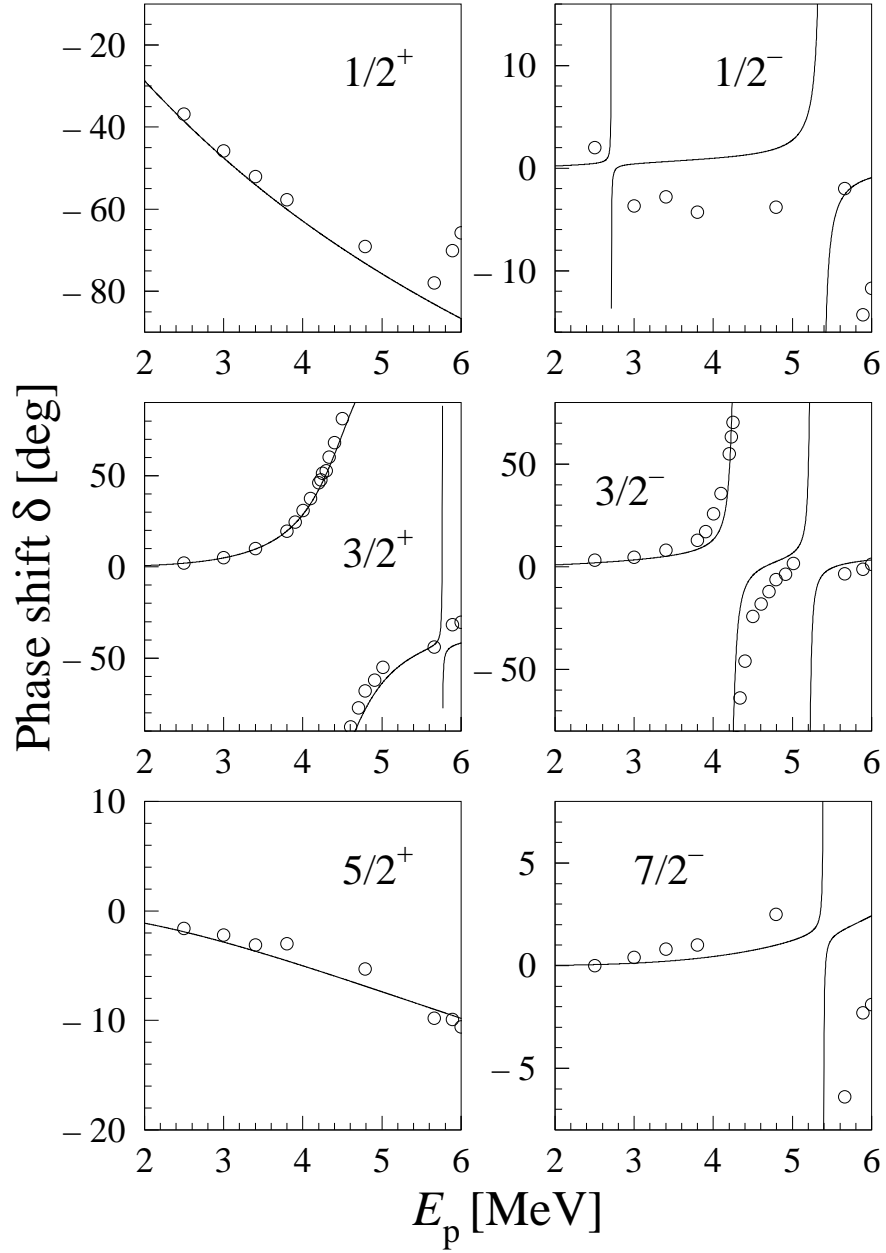


FIG. 3. The phase-shifts for the  $p+^{16}\text{O}$  elastic scattering as a function of the proton energy  $E_p$  for different partial waves. The experimental data are from [15]. SMEC results have been obtained for the ZBM effective SM interaction [3,4] and the density dependent residual interaction DDSM1 [10] (the solid line).

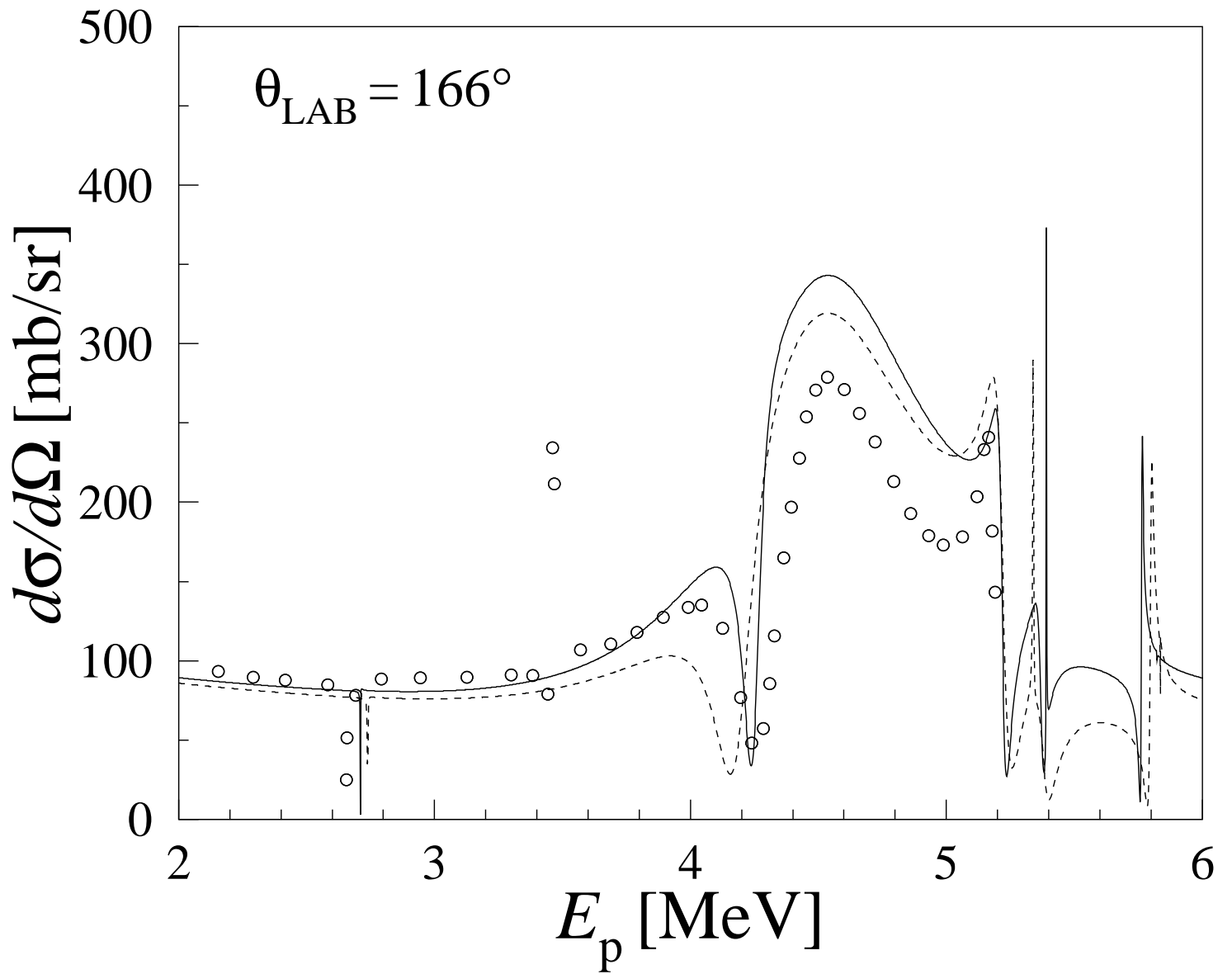


FIG. 4. The elastic cross-section at a laboratory angle  $\theta_{\text{LAB}} = 166^\circ$  for the  $p + {}^{16}\text{O}$  scattering as a function of proton energy  $E_p$ . The SMEC calculations have been performed using either DDSM0 [9] (the dashed line) or DDSM1 [10] (the solid line) residual interaction. Experimental cross-sections are from Ref. [16].